Pak. J. Chem. 15(4): 132-137, 2025 Research article

DOI: 10.15228/2025.v15.i4.p20

ISSN (Print): 2220-2625 ISSN (Online): 2222-307X

Elemental Analysis of Face Blusher Powder Using Laser Induced Breakdown

SpectroscopyA. Q. Laghari¹, N. M. Shaikh², W. A. Bhutto², A. M. Soomro², *S. Jamali³, M. A. Khoso², I. A. Sanjrani², Z. H Arain², and N. M. Laghari²

¹ Department of Physics, The Benazir Bhutto Shaheed University of Technology and Skill Development (BBSUTSD), Khairpur Mirs-66020, Sindh, Pakistan

² Institute of Physics, University of Sindh, Jamshoro 71000, Pakistan

³ Anhui Provincial Key Laboratory of Photonic Devices and Materials, Anhui Institute of Optics and Fine Mechanics, Hefei Institutes of Physical Sciences, Chinese Academy of Sciences, Hefei 230031, China

Corresponding Author: saifjamali86@yahoo.com

Abstract

The presence of toxic heavy metals in cosmetics poses significant public health risks, particularly in developing countries where regulatory oversight is limited. This study employed laser-induced breakdown spectroscopy (LIBS) to analyze elemental composition in face blusher powders. A Q-switched Nd: YAG laser (1064 nm, 6 ns pulse duration, 10 Hz repetition rate) was used to generate plasma. Results showed that 13 elements were detected, including Aluminum (Al), Barium (Ba), Calcium (Ca), Chromium (Cr), Copper (Cu), Lead (Pb), Potassium (K), Lithium (Li), Magnesium (Mg), Sodium (Na), Titanium (Ti), Zinc (Zn), and Hydrogen (H). The plasma was strongest at the beginning and weakened over time. The plasma parameters, such as electron temperature and electron number density, were determined utilizing the intensity ratio method and the Stark line broadening profile method. The electron temperature was initially recorded at 8,555 K, while the electron number density was measured at 4.69×10^{17} cm⁻³. Additionally, the plasma frequency was recorded at 6.16×10^{12} Hz.

Keywords: LIBS, Plasma Frequency, Plasma temperature, Electron number density, LIBS parameters, Face blusher

1. INTRODUCTION

The use of face blusher powder is rising globally to enhance one's look. To ensure product quality, spectroscopic analysis of the face blusher powder is essential. LIBS is a rapid spectroscopic method used for determining the elemental composition of various phases of matter, including solids, liquids, and gases, under ambient or standard atmospheric pressure conditions [1-10]. In this approach, when a laser beam strikes the target material, the atoms and ions are excited to higher energy states. The contact generates a very intense laser that forms a plasma plume from the sample. This method requires minimal or no sample preparation, in contrast to conventional research techniques.

Various research groups have already reported on the LIBS characterization of cosmetic samples. Ahmed et al. [11] employed LIBS and confirmed the presence of peaks for Sr, C, Mg, Mn, Al, Ca, Ti, Na, K, Fe, and Li. Ahmed et al. [12] studied three different Chinese blusher categories accessible in local Iraqi bazaars using LIBS, which reported the presence of Rb, Ba, Zn, Cl, Si, Mg, Ti, and Al. Gondal et al [13] identified the harmful substances in the lipstick by employing a pulse laser with an effective wavelength of 1064 nm. The contaminants included Na, C, Pb, Zn, Cr, and Cd. Abrar et al. [14] and Adepoju-Bello et al. [15] reported that the U.S. Food and Drug Administration (FDA) limits the quantity of hazardous contaminants in cosmetics. When the prescribed quantity of harmful chemicals in blush powder is exceeded through frequent use, serious health problems can develop. Lim et al. [16] studied the contaminants in cosmetics, which is concerning since exposure to these metals has been linked to detrimental consequences. However, studies have developed techniques that are not associated with cancer or an increased risk of sensitization. Quantifying and analyzing exposure to Mg, Cu, Pb, Hg, Ni, Cd, Al, Cr, Fe, As, Co, Zn, Sn, and Ti was achieved using optically correlated ablation mass spectrometry. The typical person in North America is exposed to many toxins from personal care products, some of which are detrimental to human health. The production of beauty goods is predominantly unregulated and unmonitored at the federal level; the regulation is not as stringent as it appears in society [17]. Throughout the investigation, five elements (Cu, Co, Ni, Cd, and Pb) were identified and tested on samples from various skincare categories (face wash, dry face powder, and eye shadow). These elements have demonstrated the potential to extend exposure to a source of bioaccumulation and induce severe health issues. Bocca et al [18] indicate that the following substances can induce metallic allergic contact dermatitis (MAD): Al, Au, Be, Co, Cr, Ci, Hg, Ir, Ni, Pb, Pt, Rh, and Ti. Jaishankar et al. [19] have demonstrated the impact of specific hazardous metals, including Fe, Hg, Pb, As, Cd, Al, and Cr, on the environment and human health, particularly in living organisms. Heavy metal intoxication is emerging as a significant risk factor for several health complications. Although these metals lack any biological function, they still exert toxic effects that are harmful to human health.

This study aims to conduct a spectroscopic analysis of face blusher powders utilizing laser-induced breakdown spectroscopy, as well as to characterize plasma parameters and their temporal evolution.

2.0. MATERIALS AND METHODS

2.1 Sample Collection and Sample Preparation

Face blusher samples were collected from a local market in Hyderabad, Sindh, Pakistan, and named as Sample A (Beauty Naked face blusher) and Sample B (Rivaj UK face blusher powder). The location of sample collection is illustrated in Fig. (1).



Figure 1: Geographic location of samples

The samples were generated in a pallet format across three segments. Initially, acetone was utilized to cleanse all sample handling apparatus. In the next step, 3 g of wax were mixed with 10 g of dry powder from the face blusher sample and placed in a mixer (Swing Mill HK-40) to maximize. Finally, 10 g of the mixed sample was placed in a hydraulic press and subjected to a force of 17×10^4 N to create samples in pallet format. The process is shown in Fig. (2).

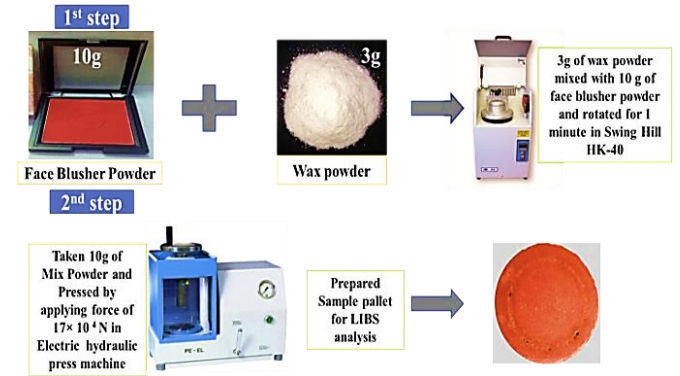


Figure 2: Methodology for preparing samples for LIBS study.

2.2 Experimental Setup

The LIBS experimental configuration is illustrated in Fig. (3). This technique employs a Q-switched Nd:YAG laser with a wavelength of 1064 nm, a pulse duration of 6 ns, and a repetition rate of 10 Hz to vaporize the sample into plasma. A quartz glass prism was employed to divert the laser beam at a 90-degree angle, so expanding the operational area and mitigating the adverse effects of the invisible laser. A quartz crystal focusing lens with a focal length of 15 cm and an optical fiber cable with a diameter of 600 nm facilitated plasma discharge from the sample surface. The DG535 delay generator was used to activate the spectrometer, creating a temporal delay between the laser pulse and the Charge-Coupled Device (CCD) camera window. A dual-channel Avantes spectrometer was utilized within a wavelength range of 300 nm to 770 nm.

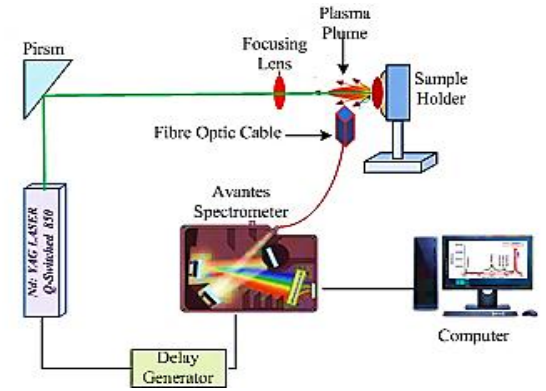


Figure 3: The LIBS apparatus arrangement

3.0 RESULTS AND DISCUSSION

3.1. Emission Spectra of Face Blusher Plasma

Th face blusher sample was ablated using Q-switched Nd: YAG laser at 1064 nm in atmospheric pressure in air. Our analysis reveals that face blusher plasma comprises the following elements: Aluminum (Al), Barium (Ba), Calcium (Ca), Chromium (Cr), Copper (Cu), Lead (Pb), Potassium (K), Lithium (Li), Magnesium (Mg), Sodium (Na), Titanium (Ti), Zinc (Zn), and Hydrogen (H). Spectral lines of the face blusher plasma emission spectrum includes Ti-I transition lines at (453.32, 454.96, and 457.19) nm Ti-II at (323.45, 323.65, 332.92, 334.90, 336.12, 337.28, 338.37, 375.92, 498.17, 499.10, 499.25, 500.72, 501.42, 501.61, 502.35, 503.99, 506.46, 595.31, 596.58, and 597.87, and 625.80) nm. Pb-I at 368.34 nm, Mg-I at (382.38, 382.93, and 383.23) nm, Ca-II lines at 393.36 nm and 396.84 nm, Ca-I at (422.67, 428.93, 430.25, 430.77, 487.81, 489.99, 493.40, 518.88, 585.74, 586.75, 610.27, 612.22, 616.21, 643.91 and 649.37) nm, Al-I at 394.0 nm and 396.15 nm, Ba-II at (455.40, 614.17) nm, K-I lines at (485.60 and 486.97,) nm, Cu-II line at 495.37 nm, Zn-II at (491.16 and 492.40) nm Mg-I at (516.73, 517.26 and 518.36) nm, Cr-I at (520.84 and 526.41), Cu-I at 521.82 nm, Na-I at 588.99 nm and 589.95 nm, H-I at 656.28 nm, Li-I at 670.79 nm, and K-I lines at 766.49 nm and 769.89 nm. The emission spectrum comprises atomic transition lines of several elements, as depicted in Fig. 4 (a – f). The NIST database used to identify the elements corresponding transition lines of face blusher powder plasma [20].

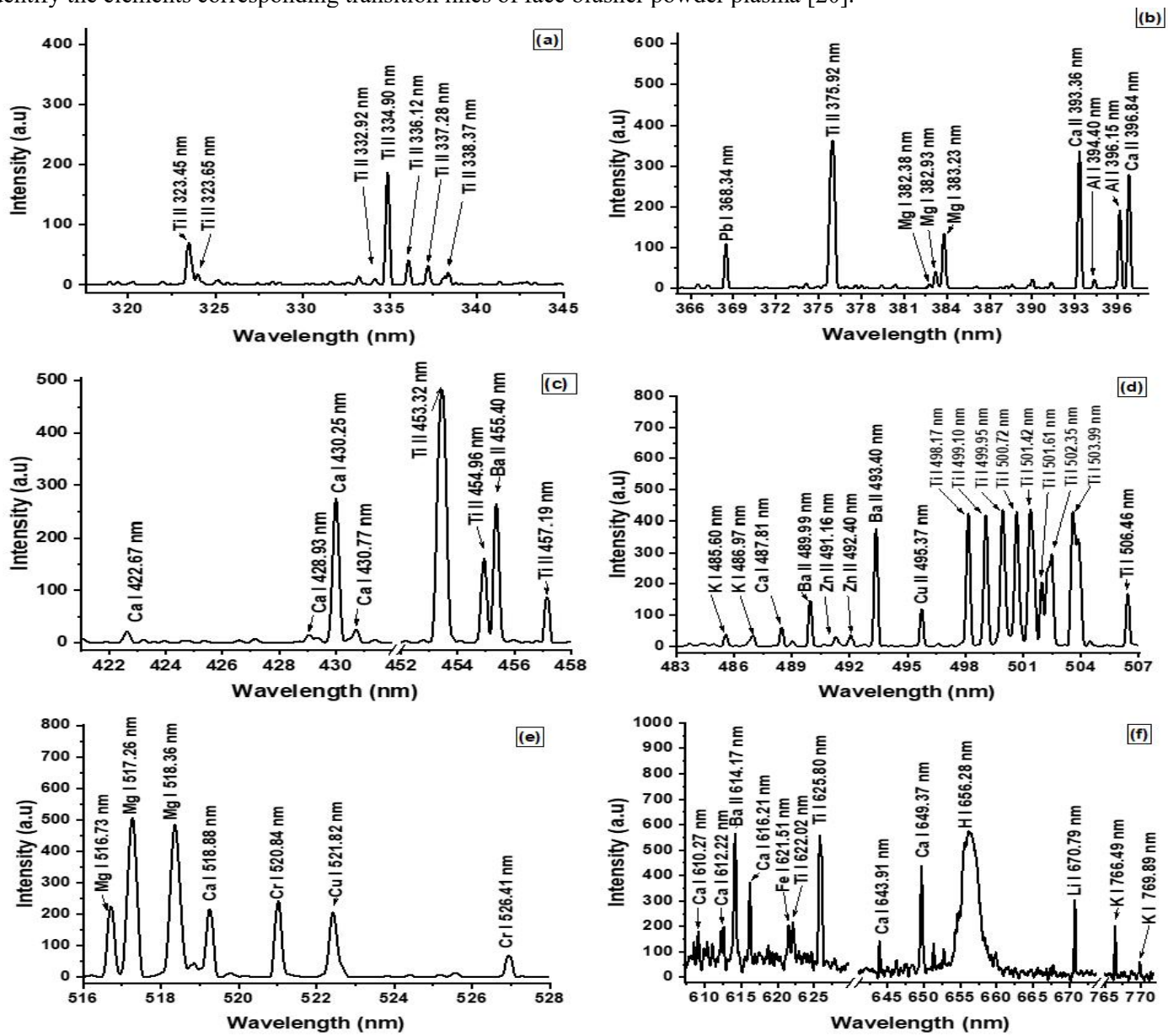


Figure 4 (a-f): Laser produced spectra of face blusher

3.2. Temporal Variation of Face Blusher Plasma

The spectra at different delay times, representative of the plasma plume, were recorded to investigate the thermodynamic behavior of the Face blusher plasma. The strength of transition lines is greater at the initial stage and decreases as the delay time increases. This occurs due to the thermalization and recombination processes that transpire in plasma over time. Fig. 5 illustrates the temporal fluctuations of barium ions at 493.40 nm.

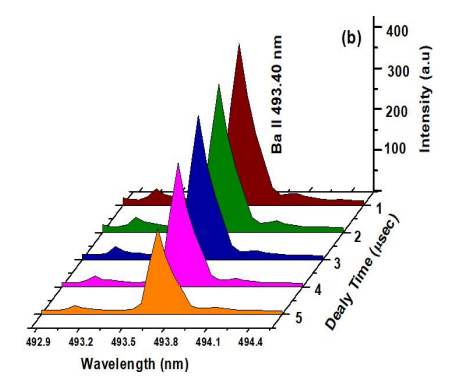


Figure 5: 3D relationship between the intensity of Ba- II Lines of face blusher powder

3.3. Plasma Parameters

3.3.1. Electron Temperature

This study employed the intensity ratio approach to ascertain the electron temperature of the plasma. This method utilizes the spectroscopic characteristics of the prominent spectral lines, encompassing wavelength, transition probability, upperlevel energy, statistical weight, and strength. The plasma temperature of the face blusher powder plasma for samples A and B is determined using Eq. (1) concerning the neutral calcium lines (Ca-I) at 430.25 nm and 616.21 nm [21], [22].

$$T_e = \frac{(E_2 - E_1)k}{k \ln \left[\frac{I_1 \lambda_1 A_2 g_2}{I_2 \lambda_2 A_1 g_1} \right]} \tag{1}$$

 $T_e = \frac{(E_2 - E_1)k}{k \ln \left[\frac{I_1 \lambda_1 A_2 g_2}{I_2 \lambda_2 A_1 g_1}\right]} \tag{1}$ Where, T_e stands for plasma temperature; E_1 and E_2 for excited energies (eV); k for Boltzmann's constant (eV.K⁻¹); A_1 and A_2 for probabilities of transition (S⁻¹); I_1 and I_2 for transition line intensities, and g for statistical weight. The electron temperature of both samples is elevated during the initial phase of plasma and diminishes as the delay period extends. Fig. (6) illustrates the temporal dynamics of electron temperature for both face blusher samples. The electron temperature of the sample is 8555 K \pm 10%. The electron temperature for sample B is 5988 K \pm 10%. The variation in electron temperature for sample A is (8555 K - 7075 K), and for sample B, it is (5988 K - 4790 K), with the variation in delay time ranging from 1.00 usec to 5.00 usec.

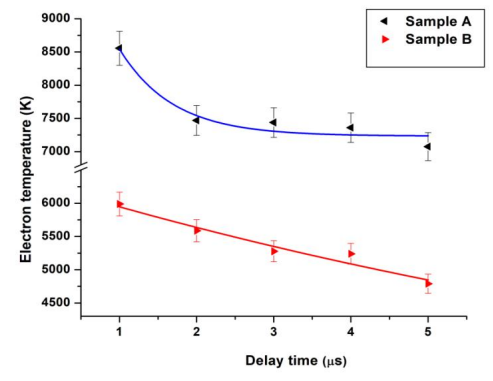


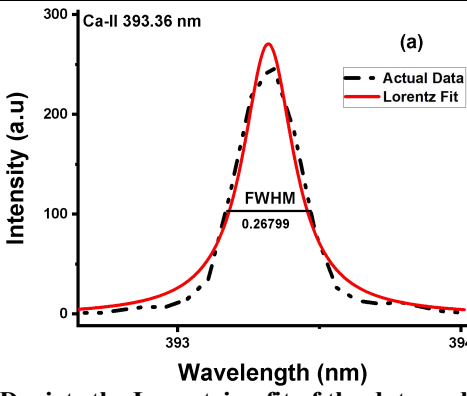
Figure 6: Variation in the electron temperature of face blusher powder at different delay durations (1–5) μsec.

3.3.2. Electron Number Density

Electron number density refers to the concentration of electrons within the plasma plume. This parameter has a significant influence on the behavior of plasma. This work calculated the electron number density using the Stark line broadening profile approach, focusing on the calcium transition line at 393.36 nm, as shown in Fig. 7(a). Electron number densities were estimated using Eq. (2) [23-25].

$$\Delta \lambda_{FWHM} = 2\omega \left(\frac{N_e}{10^{16}}\right) \tag{2}$$

 $\Delta \lambda_{FWHM} = 2\omega \left(\frac{N_e}{10^{16}}\right) \qquad (2)$ Where $(\Delta \lambda_{FWHM})$ is the full width at half maximum (nm), N_e denotes the number density (cm⁻³), and ω is a constant called the impact parameter [26]. It was observed that the electron number density is higher at the initial stage of plasma, and its values decrease as the delay time increases. In this study, the electron number density for sample A and sample B was observed as 4.69×10¹⁷ cm⁻³ and 4.62×10¹⁷ cm⁻³, respectively, at 1.00 μsec. The temporal variation of electron number density 1.00 µsec to 5.00 µsec, for sample A was observed as 4.69×10¹⁷ cm⁻³ to 4.37×10¹⁷ cm⁻³, and for sample B is observed as 4.62×10^{17} cm⁻³ and 4.11×10^{17} cm⁻³. Fig. 7(b) illustrates the variation in electron number density for both samples.



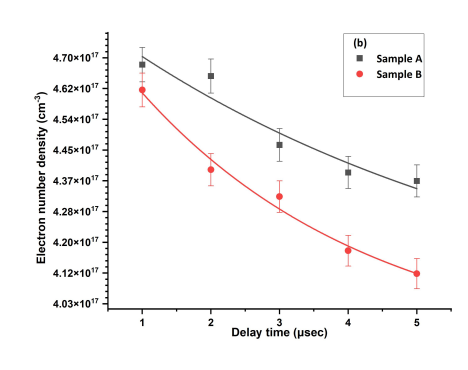


Figure 7: (a) Depicts the Lorentzian fit of the data and (b) Variation of the electron number density as a function of the delay time (1-5) µsec.

3.3.3. Plasma frequency

The abundance of species inside the plasma is a crucial measure for analyzing plasma strength. The plasma frequency (f_P) was computed using Eq. (3) in this investigation [22], [27–29].

$$f_P = 9 \times 10^3 \sqrt{N_e} \tag{3}$$

A higher plasma frequency was observed at a 1.00 µsec delay time for both samples, and its strength decreased as the delay time increased. The variation of plasma frequency for sample A was observed as $(6.16\times10^{12} - 5.95\times10^{12})$ Hz and $(6.11\times10^{12} - 5.77\times10^{12})$ Hz as the delay time increased from 1.00 µsec to 5.00 µsec. Fig. (8) illustrates the fluctuation in plasma frequency for both samples.

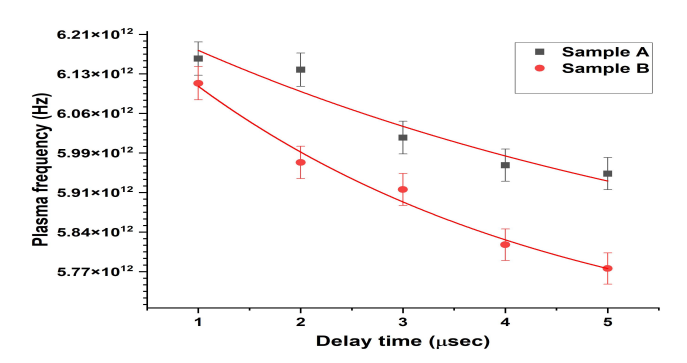


Figure 8: Display the plasma frequency variations as an outcome of time delay.

4. CONCLUSION

The study concluded that laser ablation spectroscopy is a practical method for analyzing face blusher powders, revealing the presence of multiple elemental transition lines, confrmed Aluminum (Al), Barium (Ba), Calcium (Ca), Chromium (Cr), Copper (Cu), Lead (Pb), Potassium (K), Lithium (Li), Magnesium (Mg), Sodium (Na), Titanium (Ti), Zinc (Zn), and Hydrogen (H). The results show that the intensity of transition lines, electron temperature, electron number density, and plasma frequency were highest at the initial delay time (1 μ s) and gradually decreased up to 5 μ s. The temporal variation of electron temperature ranged from 8555–7075 K for Sample A and 5988–4790 K for Sample B, while the electron number density varied between 4.69×10^{17} – 4.37×10^{17} cm⁻³ for Sample A and 4.62×10^{17} – 4.11×10^{17} cm⁻³ for Sample B. Correspondingly, the plasma frequency decreased from 6.16×10^{12} to 5.95×10^{12} Hz for Sample A and from 6.11×10^{12} to 5.77×10^{12} Hz for Sample B. Overall, these findings confirm that laser ablation spectroscopy provides a reliable and sensitive approach for elemental characterization of cosmetic powders.

Acknowledgment

We are thankful to Department of Physics, University of Agriculture Faisalabad Pakistan for providing the necessary experimental facilities in Laser Spectroscopy laboratory.

References

- 1. D. M. Silvestrem F. de O. Leme, C. S. Nomura, A. N. do Nascimento, *Microchem. J.* 126:545–550, (2016).
- 2. M. A. Gondal, Z. S. Seddigi, M. M. Nasr, B. Gondal, J. Hazard. Mater. 175(1-3):726-732, (2010).
- 3. N. M. Shaikh, S. Hafeez, B. Rashid, M. A. Baig, Eur. Phys. J. D 44(2):371–379, (2007).
- 4. Y. Tian, H. C. Cheung, R. Zheng, Q. Ma, Y. Chen, N. Delepine-Gilon, Y. Jin, *Spectrochim. Acta B* 124:16–24, (2016).
- 5. K. Rehan, I. Rehan, S. Sultana, M. Z. Khan, Z. Farooq, A. Mateen, M. Humayun, *Int. J. Spectrosc.* 2017:1–9, (2017).
- 6. J. Iqbal, R. Ahmed, M. Rafique, M. Anwar-Ul-Haq, M. A. Baig, Laser Phys. 26(7):076001, (2016).

- 7. T. Takahashi, B. Thornton, *Spectrochim. Acta B* 138:31–42, (2017).
- 8. D. A. Cremers, L. J. Radziemski, Handb. Laser-Induced Breakdown Spectrosc., (2013).
- 9. J. N. Okereke, A. C. Udebuani, E. U. Ezeji, K. O. Obasi, M. C. Nnoli, Science, 3(5-1):358-63, (2015).
- 10. S. Jamali, N. M. Shaikh, M. A. Khoso, Y. Jamil, W. A. Bhutto, A. M. Soomro, R. H. Mari, *Optik* 261:169246, (2022).
- 11. M. F. Ahmed, K. M. Abdein, M. E. Sadat, A. I. Talunkder, M. Wahadoszamen, A. F. Haider, *J. Bangladesh Acad. Sci.* 33(2):209–218, (2009).
- 12. A. Ahmed, M. Salman, M. Alwazzan, A. Meri, J. Cosmet. Sci. Res. (2)1-8, (2019).
- 13. M. A. Gondal, Z. S. Seddigi, M. M. Nasr, B. Gondal, J. Hazard. Mater. 175(1-3):726-732, (2010).
- 14. M. Abrar, T. Iqbal, M. Fahad, M. Andleeb, Z. Farooq, S. Afsheen, Laser Phys. 28(5):055601, (2018).
- 15. A. A. Adepoju-Bello, O. O. Oguntibeju, R. A. Adebisi, N. Okpala, H. A. B. Coker, *Afr. J. Biotechnol.* **11**(97):16360–16364, **(2012)**.
- D. S. Lim, T. H. Roh, M. K. Kim, Y. C. Kwon, S. M. Choi, S. J. Kwack, K. B. Kim, S. Yoon, H. S. Kim, B. Lee, J. Toxicol. Environ. Health A 81(11):432–452, (2018).
- 17. S. H. Khazaal, Engg. & Tech. J. 35(2), (2017).
- 18. B. Bocca, G. Forte, Open Chem. Biomed. Methods J. 2(2):26–34, (2009).
- 19. M. Jaishankar, T. Tseten, N. Anbalagan, B. B. Mathew, K. N. Beeregowda, *Interdiscip. Toxicol.* 7(2):60–72, (2014).
- 20. J. E. Sansonetti, W. C. Martin, J. Phys. Chem. Ref. Data 34(4):1559–2259, (2005).
- 21. Q. Li, A. Chen, D. Zhang, Q. Wang, W. Xu, Y. Qi, S. Li, Y. Jiang, M. Jin, *Optik* 225:165812, (2021).
- 22. S. Jamali, M. A. Khoso, M. H. Zaman, Y. Jamil, W. A. Bhutto, A. Abbas, R. H. Mari, M. S. Kalhoro, N. M. Shaikh, *Phys. B Condens. Matter* 620:413278, (2021).
- 23. A. Safeen, W. H. Shah, R. Khan, A. Shakeel, Y. Iqbal, G. Asghar, R. Khan, G. Khan, K. Safeen, W. Shah, *Dig. J. Nanomater. Biostruct.* 14(1):29–35, (2019).
- 24. G. Murtaza, N. M. Shaikh, G. A. Kandhro, M. Ashraf, Spectrochim. Acta A 223:117374, (2019).
- 25. X. F. Li, W. D. Zhou, Z. F. Cui, Front. Phys. 7(6):721–727, (2012).
- 26. N. Konjević, A. Lesage, J. R. Fuhr, W. L. Wiese, J. Phys. Chem. Ref. Data 31(3):819–927, (2002).
- 27. W. S. Hussein, A. F. Ahmed, *Iraqi J. Phys.* 17(42):103–107, (2019).
- 28. E. Apaydin, M. Celik, Spectrochim. Acta B 160:105673, (2019).
- 29. B. M. Ahmed, IOP Conf. Ser. Mater. Sci. Eng. 928(7):072096, (2020).

Received: October 20th 2025 Accepted: November 3nd 2025